ADVANCES IN ATMOSPHERIC SCIENCES, VOL. 35, OCTOBER 2018, 1254–1264

• **Original Paper** •

Impact of Global Oceanic Warming on Winter Eurasian Climate

Xin HAO*[1,6,4,2], Shengping HE[5,2,1,3], Tingting HAN[1,2,3,4], and Huijun WANG[3,1,2,4]

[1]*Nansen-Zhu International Research Center, Institute of Atmospheric Physics Chinese Academy of Sciences, Beijing* 100029*, China*

[2]*Climate Change Research Center, Chinese Academy of Sciences, Beijing* 100029*, China*

[3]*Collaborative Innovation Center on Forecast and Evaluation of Meteorological Disasters/Key Laboratory of Meteorological Disaster, Ministry of Education, Nanjing University of Information Science & Technology, Nanjing* 210044*, China*

[4]*University of Chinese Academy of Sciences, Beijing* 100029*, China*

[5]*Geophysical Institute, University of Bergen and Bjerknes Centre for Climate Research, Bergen* 0025*, Norway*

[6]*Joint Center for Global Change Studies (JCGCS), Beijing* 100875*, China*

(Received 6 September 2017; revised 28 February 2018; accepted 11 April 2018)

ABSTRACT

In the 20th century, Eurasian warming was observed and was closely related to global oceanic warming (the first leading rotated empirical orthogonal function of annual mean sea surface temperature over the period 1901–2004). Here, large-scale patterns of covariability between global oceanic warming and circulation anomalies are investigated based on NCEP–NCAR reanalysis data. In winter, certain dominant features are found, such as a positive pattern of the North Atlantic Oscillation (NAO), low-pressure anomalies over northern Eurasia, and a weakened East Asian trough. Numerical experiments with the CAM3.5, CCM3 and GFDL models are used to explore the contribution of global oceanic warming to the winter Eurasian climate. Results show that a positive NAO anomaly, low-pressure anomalies in northern Eurasia, and a weaker-than-normal East Asian trough are induced by global oceanic warming. Consequently, there are warmer winters in Europe and the northern part of East Asia. However, the Eurasian climate changes differ slightly among the three models. Eddy forcing and convective heating from those models may be the reason for the different responses of Eurasian climate.

Key words: global oceanic warming, Eurasian warming, convective heating

Citation: Hao, X., S. P. He, T. T. Han, and H. J. Wang, 2018: Impact of global oceanic warming on winter Eurasian climate. *Adv. Atmos. Sci.*, **35**(10), 1254–1264, https://doi.org/10.1007/s00376-018-7216-5.

1. Introduction

Global warming is noticeable over a wide range of time scales. A vigorous and continuous rise in sea surface temperature (SST) and land surface temperature has been caused by increasing greenhouse gases during the last century (e.g., Hansen et al., 2010; Xie et al., 2010). Shin and Sardeshmukh (2011) found that the recent rising trend of surface air temperature (SAT) over land masses surrounding the North Atlantic Ocean could be captured by models, with oceanic warming observed in the tropics but not with observed radiative forcing changes. This is similar to the results of many studies (e.g., Schneider et al., 2003; Hurrell et al., 2004; Herweijer and Seager, 2008). Several studies have suggested that the direct land temperature response to radiative forcing is much smaller than the response to SST anomalies induced by radiative forcing (Schneider et al., 2003; Bracco et al., 2004; Deser et al., 2004; Hoerling et al., 2008). These evidence-based results show the importance of oceanic warming in climate change research under a CO_2-enriched atmosphere.

Many studies have demonstrated that variations of Indian Ocean and North Atlantic Ocean SSTs are important in Eurasian climate. The North Atlantic Oscillation (NAO) is known to have a link with a tripolar SST anomaly in the North Atlantic, which causes large changes in surface temperature and precipitation over Eurasia (Frankignoul, 1985; Wallace et al., 1990; Frankignoul et al., 1998; Watanabe and Kimoto, 2000; Visbeck et al., 2003). Hoerling et al. (2004) and Hurrell et al. (2004) revealed a nonlinear response of the winter NAO to tropical oceanic warming, implying a mechanism of oceanic warming with an influence on European climate change. The variations of Indian Ocean SST affect the strength and location of the sea level pressure field over the western North Pacific, which may influence the intensity of the northeast East Asian winter monsoon (Hu and Huang, 2011; Ueda et al., 2015). Li et al. (2008) indicated a prominent warming in the Indian Ocean, which intensifies the East Asian summer monsoon with an enhanced South Asian high, in agreement with Hu (1997) and Hu et al. (2003).

* Corresponding author: Xin HAO
Email: haoxlike91@163.com

In the period 1901–2004, trends of annual mean SST show prominent increases in the Atlantic and Indian oceans (Fig. 1). However, it is still unclear what effect global oceanic warming had on Eurasian climate over the 20th century. In this study, we focus on the contribution of global oceanic warming to winter Eurasian climate change, using a series of model simulations.

2. Data and methods

We acquired monthly and daily meteorological data from the NCEP–NCAR reanalysis dataset (Kalnay et al., 1996), and observational SAT data from the CRU TS3.2 dataset (Mitchell and Jones, 2005). Numerical experiments were performed by the U.S. CLIVAR drought working group. Using Met Office Hadley Centre SST datasets (Rayner et al., 2003), that working group used rotated empirical orthogonal function (REOF) analysis of annual mean SST over the period 1901–2004, based on varimax rotation. As a result, the first leading mode of annual mean SST anomalies displayed long-term warming of global SST. It revealed that a rapid increase in global SST occurred during 1925–1945 and 1960–2000. The global oceanic warming pattern was scaled by the standard deviation of its associated principal component (PC; Fig. 1b) to produce a magnified SST anomaly (Fig. 1a). The working group added this magnified SST anomaly to the monthly SST climatology (defined for 1901–2004) to be a prescribed SST. The GFDL (Delworth et al., 2006), CAM3.5 (http://www.ccsm.ucar.edu/models/atm-cam/) and CCM3 (Kiehl et al., 1998) models were forced by the prescribed SST, which was abbreviated as the LTw run. Additionally, the three models were forced by monthly SST climatology, referred to as the control run. The SST forcing was repeated with no interannual variability in each experiment. Details of the three models are shown in Table 1. The aim was to investigate the impact of long-term oceanic warming on the Eurasian climate. Hence, we analyzed the difference between the LTw and control runs. Each run spun up for more than 51 years, and data of the last 45 years were used.

The storm tracks used in our study were defined by Lau (1988). Daily data of geopotential height were used with a bandpass filter to obtain fluctuations with 2.5–6-day periods, and then filtered time series of geopotential height were split into individual seasonal segments, one for winter (December–January–February). For each seasonal segment, its mean values were subtracted from the filtered daily data of the same winter, and temporal root-mean-square values were then computed for that segment.

3. Results

The time series of wintertime Eurasian SAT and global oceanic warming, describing Eurasian SAT and global SST, continually increased during the 20th century (Fig. 2). The

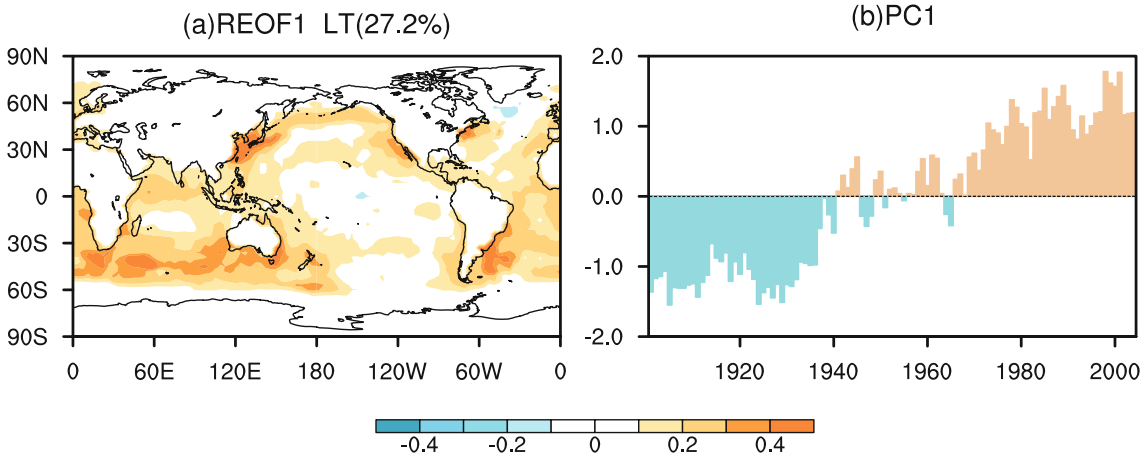

Fig. 1. First leading REOF (a) and associated PC1 (b) of annual mean SST based on the period 1901–2004. This mode is the long-term warming oceans, which was divided by a factor of two to add to the monthly SST climatology in the models.

Table 1. Description of the three models used in this study.

Model	Resolution	Convection scheme	Land surface model
CAM3.5	Approximately 1.9° (lat) ×2.5° (lon), with 27 hybrid sigma levels	Zhang–McFarlane scheme (Zhang and McFarlane, 1995)	Community Land Model (Oleson et al., 2008)
GFDL AM2.1	2° (lat) ×2.5° (lon), L24	Relaxed Arakawa–Schubert (Moorthi and Suarez, 1992)	Milly and Shmakin (2002)
CCM3	Approximately 2.8° (lat) ×2.8° (lon), with 18 hybrid sigma levels	Zhang–McFarlane scheme (Zhang and McFarlane, 1995)	Bonan (1996)

wintertime Eurasian warming had a close relationship with global oceanic warming. Their correlation coefficient is 0.52 for the period 1901–2004. To confirm the connection between the Eurasian climate and long-term oceanic warming in winter, we further regressed the atmospheric circulation against PC1 for 1948–2004 (Fig. 3). The regression map of sea level pressure (SLP) is characterized by a negative anomaly covering the high-latitude North Atlantic and an opposite-sign anomaly in the midlatitude North Atlantic (Fig. 3a). This dipolar pattern resembles a positive pattern of the NAO. We also found that global oceanic warming was accompanied by low-pressure anomalies over the northern Eurasian continent and the Aleutian Islands (Fig. 3a). The regression result of 500-hPa geopotential height shows a positive NAO anomaly and a weakened East Asian trough (Fig. 3c). Thus, in the lower troposphere, anomalous westerly wind over Europe and anomalous southerly wind over East Asia, which bring more humid and warmer air to the Eurasian continent,

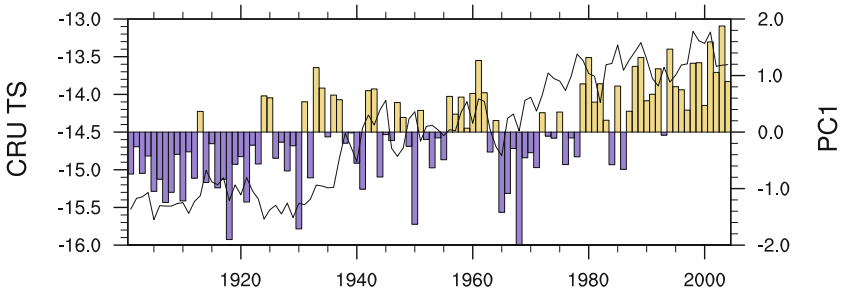

Fig. 2. Winter-mean surface temperature average over Eurasian region based on CRU TS3.2 dataset (bars; units: °C) and the PC1 associated with REOF1 (line), for the period 1901–2004.

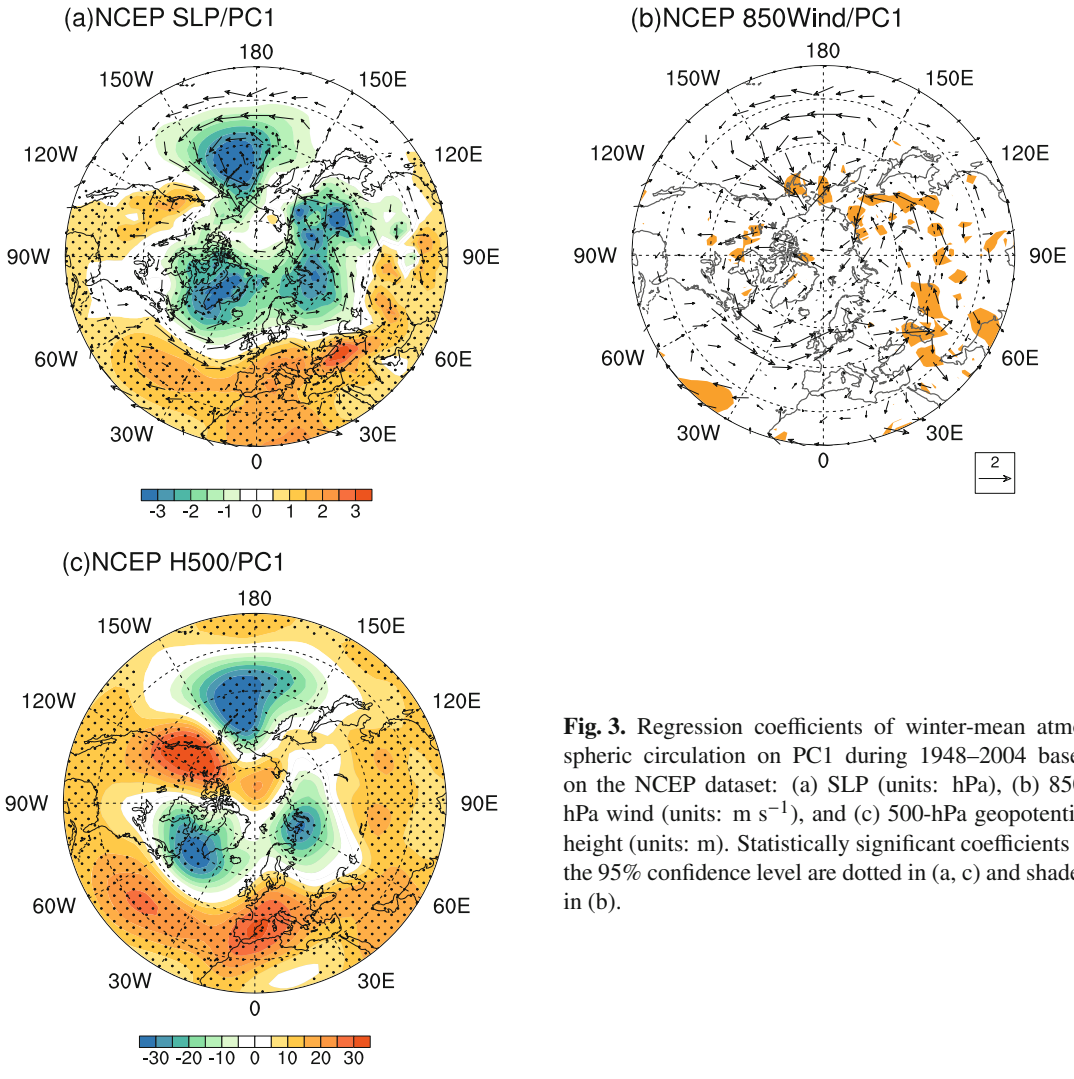

Fig. 3. Regression coefficients of winter-mean atmospheric circulation on PC1 during 1948–2004 based on the NCEP dataset: (a) SLP (units: hPa), (b) 850-hPa wind (units: m s^{-1}), and (c) 500-hPa geopotential height (units: m). Statistically significant coefficients at the 95% confidence level are dotted in (a, c) and shaded in (b).

are clearly correlated with global oceanic warming (Fig. 3b). This favors warmer winters in Eurasia.

The general consensus has been that the upward trend of winter NAO involves synoptic eddy feedbacks associated with changes in the North Atlantic storm track (Wallace et al., 1990; Watanabe and Kimoto, 2000; Hoerling et al., 2004; Hurrell et al., 2004; Cohen and Barlow, 2005). The NAO generates a North Atlantic horseshoe pattern and, in turn, an NAO-like response primarily results from perturbations in the Atlantic storm track caused by subpolar and midlatitude forcing in winter (Sutton et al., 2000; Czaja and Frankignoul, 2002; Peng et al., 2003; Gastineau and Frankignoul, 2015). Hoerling et al. (2004) and Hurrell et al. (2004) suggested that changes in tropical rainfall, especially forced by Indian Ocean warming, also contribute to a winter NAO response. The global oceanic warming pattern is not only characterized by tropical warming but also by a negative center over the Labrador Sea and an opposite-sign anomaly in the midlatitude North Atlantic, which is somewhat similar to the extratropical portion of the SST anomaly tripole. From linear regression, precipitation and midlatitude storm track anomalies are significantly associated with global oceanic warming (Fig. 4). As results show, the storm track over the midlatitude North Atlantic and precipitation over the North Atlantic and tropics have apparent perturbations related to long-term oceanic warming, which can sustain dipolar anomalous eddy forcing for the positive NAO-like atmospheric response (Fig. 4; Peng et al., 2003; Hoerling et al., 2004; Hurrell et al., 2004). Additionally, we found that the storm tracks associated with global oceanic warming obviously increased in midlatitude East Asia, corresponding to a strengthened East Asian trough. We also found that precipitation over Russia was enhanced in the last century (Fig. 4), which implies low-pressure anomalies over the northern Eurasian continent may involve diabatic heating associated with the changes in rainfall.

The key question is: what was the contribution of global oceanic warming to the aforementioned circulation anomalies, which led to the Eurasian surface temperature rise in the recent warming period? To examine the impact of global oceanic warming on the Eurasian climate during boreal winter, idealized SST experiments were performed using three atmospheric general circulation models. Figure 5 shows the response of SLP and 850-hPa wind to global oceanic warming in winter. The outstanding characteristics of the boreal winter SLP response in all three models are low-pressure anomalies over Iceland and northern Eurasia and high-pressure anomalies over the subtropical North Atlantic (Fig. 5). Additionally, there was a remarkable weaker-than-normal Aleutian low (AL) and a low-pressure anomaly over northern Eurasia caused by global oceanic warming (Fig. 5). In the mid-troposphere, geopotential height anomalies were characterized by a dipolar anomaly over the North Atlantic, with a positive center around (40°N, 10°W) and a negative center over north of 60°N (Fig. 6). The response of 500-hPa geopotential height in the East Asia–Pacific sector featured a weakened East Asian trough (Fig. 6). The dipolar modes of the SLP and geopotential height anomalies over the North

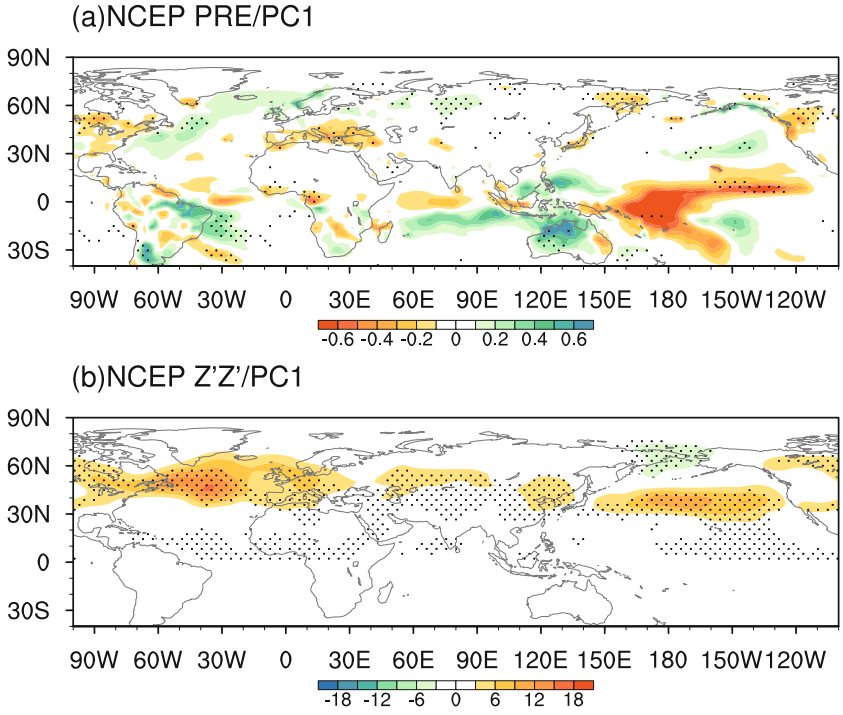

Fig. 4. Regression coefficients of winter-mean atmospheric circulation on PC1 during 1948–2004 based on the NCEP dataset: (a) precipitation rate (units: mm d^{-1}) and (b) 250-hPa storm track (units: m^2). Statistically significant coefficients at the 95% confidence level are dotted.

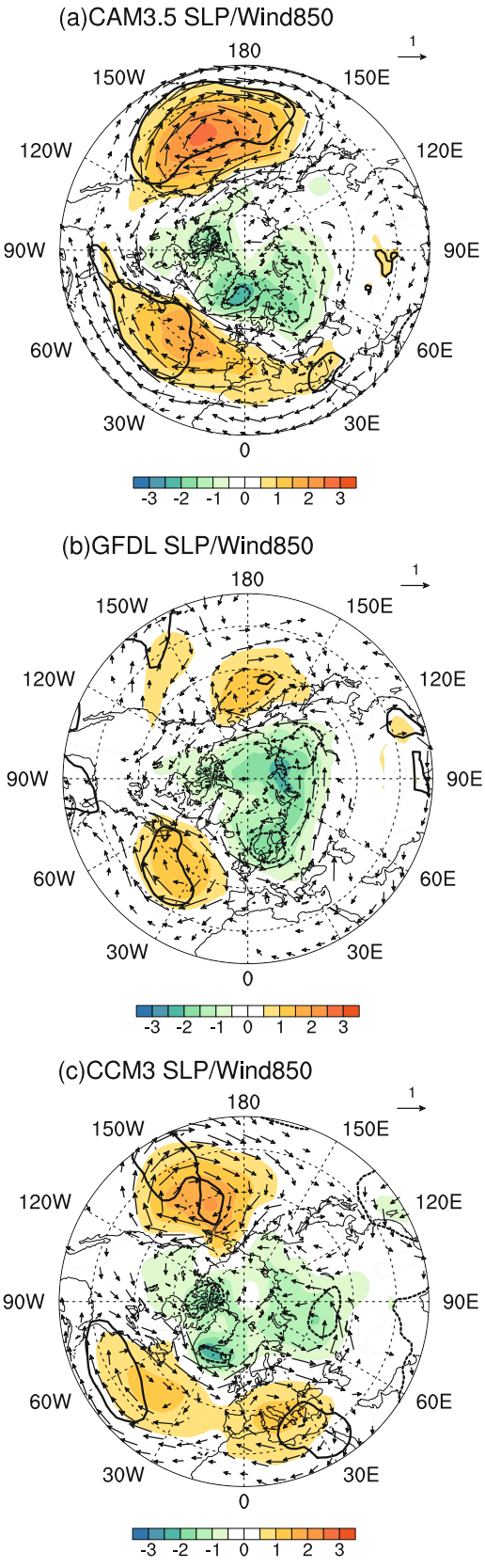

Fig. 5. Difference in SLP (color shading; units: hPa) and 850-hPa winds (vectors; units: m s^{-1}) between the LTw and control runs from (a) CAM3.5, (b) GFDL and (c) CCM3. The black lines indicate the 90% confidence levels (positive, solid line; negative, dashed line).

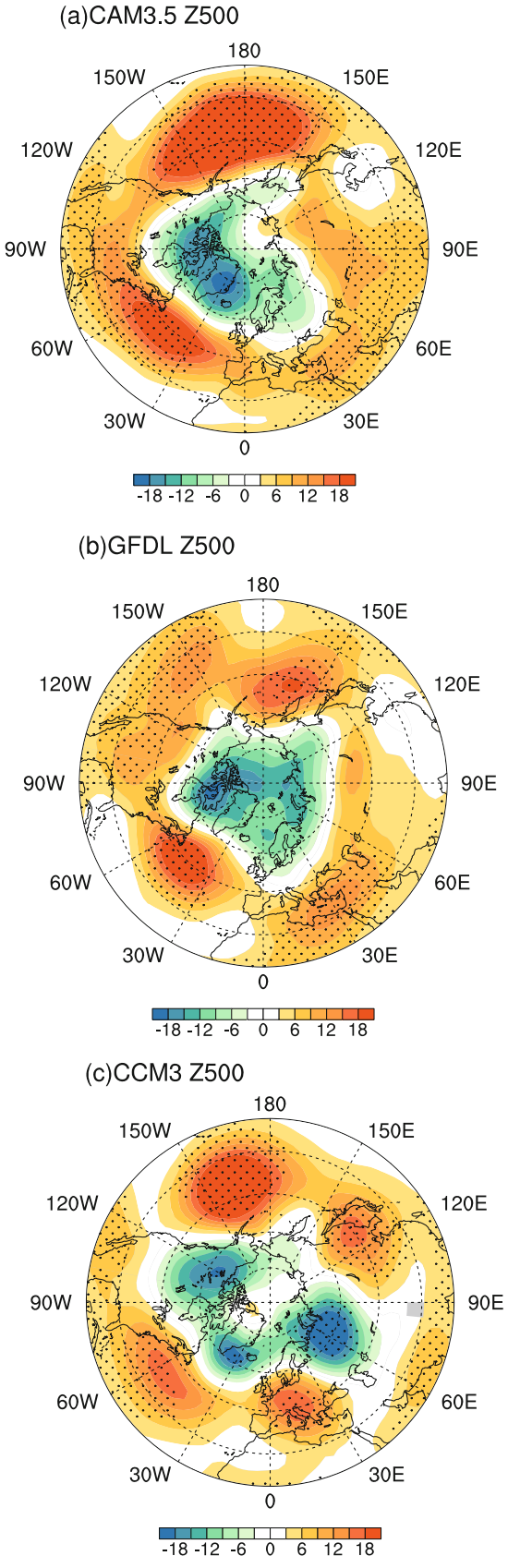

Fig. 6. Difference in 500-hPa geopotential height (units: m) between the LTw and control runs from (a) CAM3.5, (b) GFDL and (c) CCM3. Stippled areas indicate the 90% confidence level.

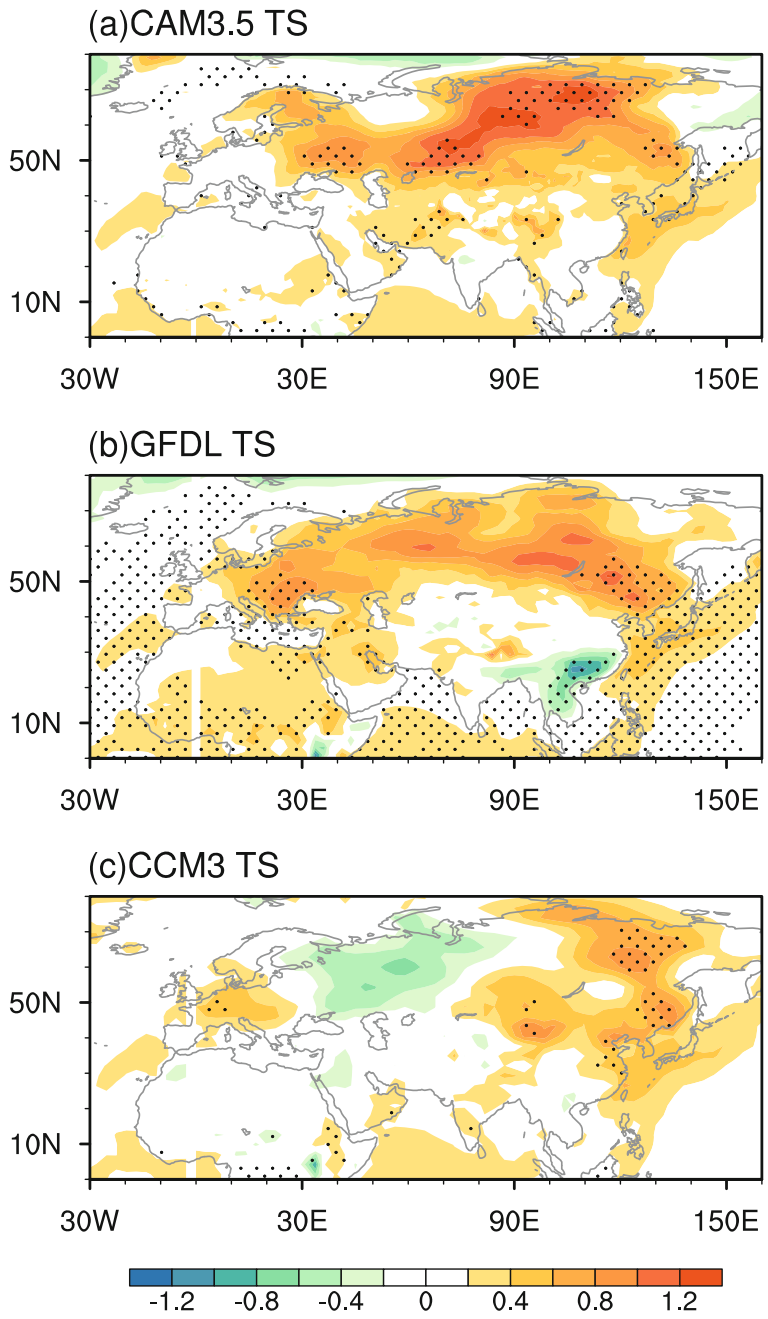

Fig. 7. Difference in SAT (units: °C) between the LTw and control runs from (a) CAM3.5, (b) GFDL and (c) CCM3. Stippled areas indicate the 90% confidence level.

Atlantic resemble the positive pattern of the NAO pattern, which was accompanied by anomalous westerlies over Europe (Figs. 5 and 6), leading to wet and warm conditions there (Fig. 7; Glowienka-Hense, 1990; Rodwell et al., 1999). The low-pressure anomaly over northern Eurasia and weakened East Asian trough drove anomalous southeasterly flow in the coastal areas of midlatitude East Asia, thereby obstructing cold and dry air penetration of East Asia (Figs. 5 and 7). These results indicate that the spatial patterns of circulation change over the North Atlantic and Eurasia are consistent with the dynamic response of atmospheric circulation to global oceanic warming. However, global oceanic warming appears not to be of primary importance for AL variability.

It is remarkable that SAT responses varied among the three models. The response in CAM3.5 shows strong positive anomalies over the entire Eurasian continent. The response in GFDL has a different feature, i.e., significant negative anomalies in the southern part of East Asia. In the CCM3 model, the SAT clearly increases in East Asia and Europe, but the decrease in SAT over western Russia is different from the responses in CAM3.5 and GFDL. Based on the assessments by Magnusdottir (2001) and Hao et al. (2016), we consider that, compared to CAM3.5 and GFDL, the response of the Eurasian climate to SST anomalies is quite well represented

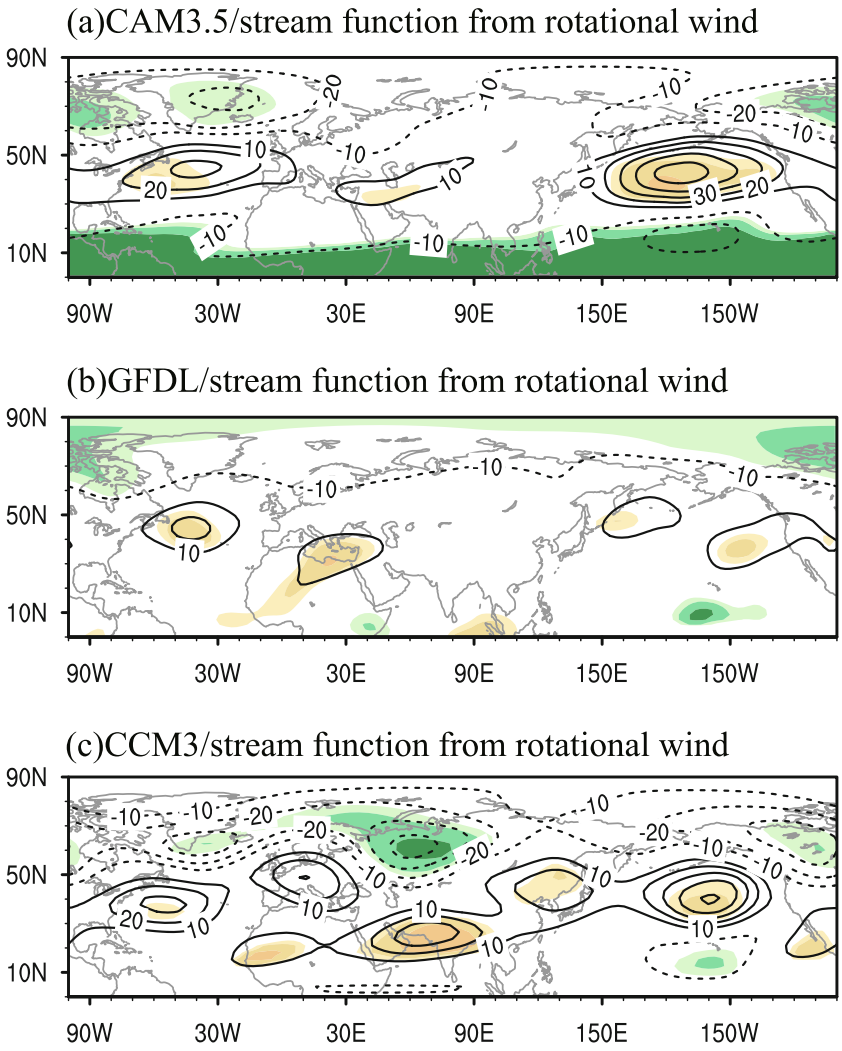

Fig. 8. Difference in the 950–250-hPa average streamfunction (units: 10^5 m^2 s^{-1}), calculated from rotational wind, between the LTw and control runs from (a) CAM3.5, (b) GFDL and (c) CCM3. Light, medium, and dark shading indicates the 90%, 95% and 99% confidence levels (positive, yellow; negative, green), respectively.

in CCM3.

The positive pattern of the NAO, weaker-than-normal East Asian trough, and low-pressure anomaly in Eurasia played key roles in the responses of Eurasian SAT. From the above discussion, comparison with other studies suggests that eddy forcing associated with storm tracks and diabatic heating causes the change in the NAO (Peng et al., 2003; Hoerling et al., 2004; Hurrell et al., 2004). Figure 8 shows the 950–250-hPa average streamfunction differences between the LTw and control runs, calculated from rotational winds. The anomalous 950–250-hPa average streamfunction, which is associated with stationary eddy vorticity forcing, exhibits an obvious dipole over the North Atlantic Ocean from the three models (Fig. 8). The strongest (weakest) 950–250-hPa average streamfunction anomalies in CAM3.5 (GFDL) correspond to the strongest (weakest) NAO response. Strong similarity between those anomalies and 500-hPa geopotential height over the East Asia–Pacific sector implies that the weakened East Asian trough may be driven by the eddy forcing. Berckmans et al. (2013) suggested that blocking frequency in the Europe and Pacific sector is increased at high resolution, which means that eddy forcing is increased. They also found that improvement in the resolution of orography actually reduces blocking. Thus, we consider that the resolution and land surface model used in the three models may be responsible for the different circulation responses associated with eddy forcing.

Nevertheless, 200-hPa velocity potential differences between the LTw and control runs reveal that global oceanic warming can induce divergence anomalies over the Indian Ocean and Eurasia, as well as anomalous convergence over the North Pacific (Fig. 9). The anomalous divergence centered over Eurasia is favorable for generating a low-pressure anomaly over northern Eurasia (Figs. 5 and 9). The convection scheme in a model determines the spatial distribution of convective heating (Gregory and Rowntree, 1990). Figure 10

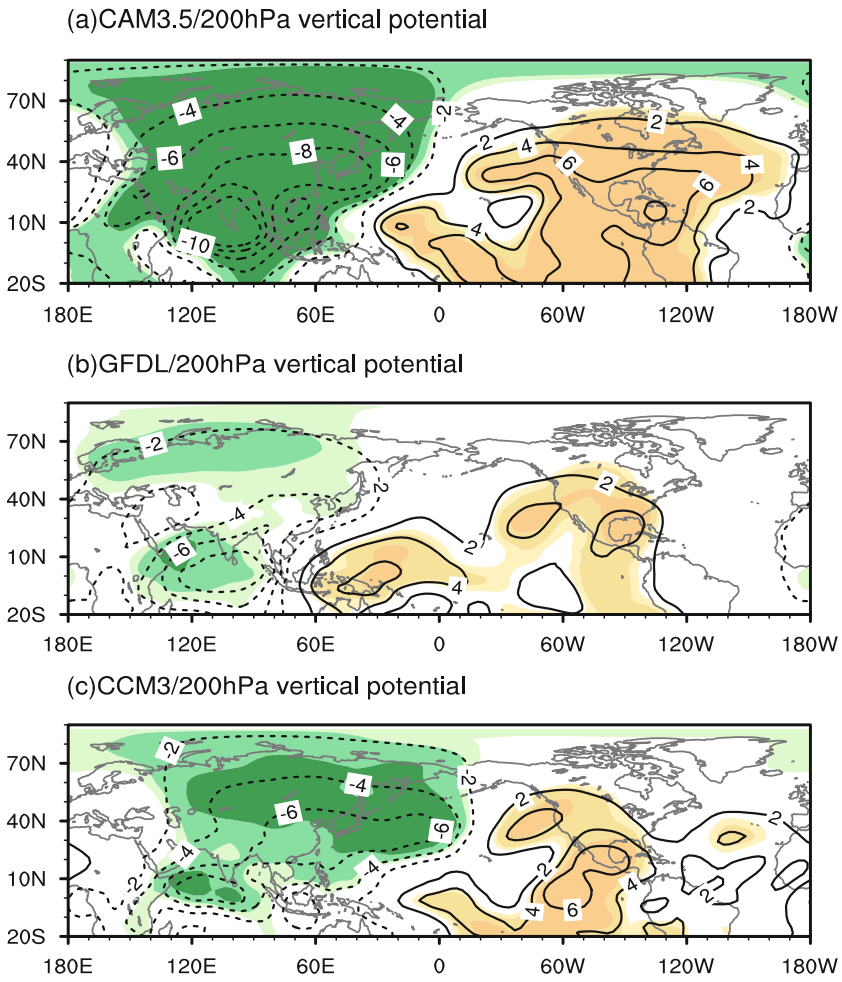

Fig. 9. Difference in the 200-hPa velocity potential (units: 10^5 m^2 s^{-1}) between the LTw and control runs from (a) CAM3.5, (b) GFDL and (c) CCM3. Light, medium and dark shading indicate the 90%, 95% and 99% confidence levels (positive, yellow; negative, green), respectively.

shows precipitation differences between the LTw and control runs. The tremendous differences in precipitation responses among the three models show discrepancies in convective heating driven by global oceanic warming. As a consequence, the intensity and location of the low-pressure anomaly over northern Eurasia are different among the three models.

4. Conclusions

During winter, Eurasian SAT increased substantially in the 20th century, and its time series shows a strong relationship with global oceanic warming. Based on reanalysis datasets, we investigated the relationship between atmospheric circulation and global oceanic warming during winter. We discovered a robust and highly significant association between the NAO and global oceanic warming. Additionally, accompanied by global oceanic warming, there was a low-pressure anomaly over northern Eurasia and a weakened East Asian trough.

We thus explored whether global oceanic warming was a contributor to Eurasian climate change in the last century, using numerical experiments with CAM3.5, GFDL and CCM3. We found that atmospheric circulation responses in the three models to global oceanic warming were generally in agreement. An anomalous dipole with a positive center around (40°N, 10°W) and a negative center north of 60°N was seen in both the SLP anomaly field and 500-hPa geopotential height anomaly field, resembling the NAO positive phase. The positive NAO-like response resulted in warm winters in northern Europe. Furthermore, in response to global oceanic warming, a low-pressure anomaly in northern Eurasia and a weaker-than-normal East Asian trough occurred and obstructed southward cold air intrusion, leading to warm winters in East Asia.

The Eurasian climate response was slightly different among the three models. Previous studies considered eddy forcing and convective heating as primary contributors to winter atmospheric circulation responses (Watanabe and Kimoto, 2000; Hoerling et al., 2004; Hurrell et al., 2004; Cohen and Barlow, 2005). In the three models, the vertically averaged streamfunction responses associated with stationary

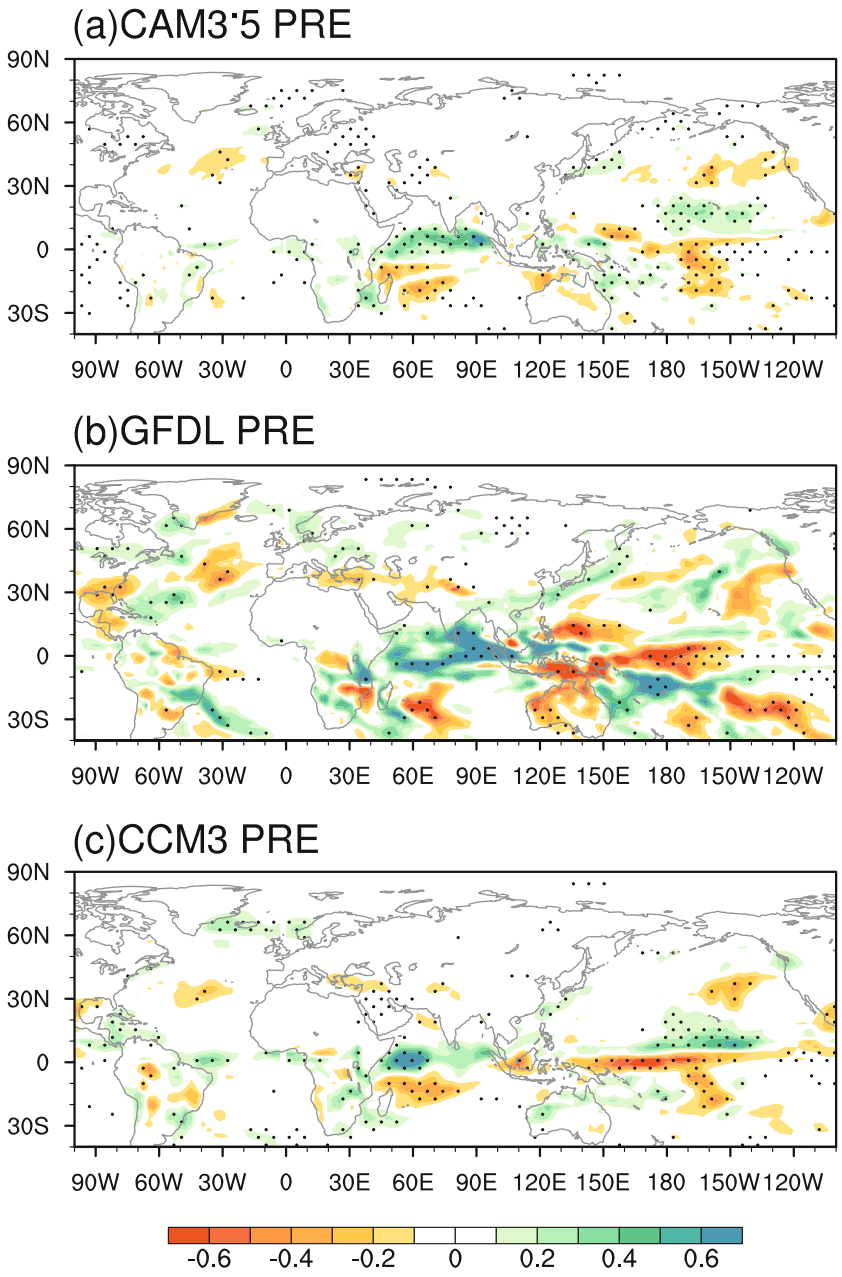

Fig. 10. Difference in the precipitation rate (units: mm d^{-1}) between the LTw and control runs from (a) CAM3.5, (b) GFDL and (c) CCM3. Stippled areas indicate the 90% confidence level.

eddy forcing show an obvious dipolar pattern in the North Atlantic and a positive center in the midlatitude East Asia–Pacific region, but with different intensities. Consequently, the intensity of the NAO-like response and East Asian trough response varies across the models. Divergence over Eurasia forced by global oceanic warming induces a low-pressure anomaly over northern Eurasia. The intensity of the divergence over Eurasia induced by convective heating is also different among the three models. In summary, the varying intensities of circulation responses cause different SAT responses among these models.

Note that the AL intensity strengthened during the last century (Fig. 3a), which has been identified as a consequence of anthropogenic warming and natural variability (Gan et al., 2017). Nevertheless, the AL response to global oceanic warming was inconsistent with the AL variability computed from the reanalysis dataset. This implies that global oceanic warming might make a small contribution to AL variability.

Acknowledgements. This research was supported by the National Key Research and Development Program of China (Grant No. 2016YFA0600703), the National Science Foundation of China (Grant No. 41421004), and the Chinese Academy of Sciences–Peking University (CAS–PKU) partnership program. This research

was also supported by "the Fundamental Research Funds for the Central Universities". The work was partially supported by the U.S. CLIVAR drought working group activity for coordinating and comparing climate model simulations forced by a common set of idealized SST patterns. We thank the Lamont-Doherty Earth Observatory of Columbia University for making their CCM3 runs available, NOAA's Geophysical Fluid Dynamics Laboratory for the AM2.1 (GFDL) runs, and the National Center for Atmospheric Research for the CAM3.5 runs.

REFERENCES

Berckmans, J., T. Wollings, M.-E. Demory, P.-L Vidale, and M. Roberts, 2013: Atmospheric blocking in a high resolution climate model: influences of mean state, orography and eddy forcing. *Atmospheric Science Letters*, **14**, 34–40, https://doi.org/10.1002/asl2.412.

Bonan, G. B., 1996: The NCAR land surface model (LSM version 1.0) coupled to the NCAR community climate model. NCAR Tech. Rep. NCAR/TN-429 + STR, 171 pp.

Bracco, A., F. Kucharski, R. Kallummal, and F. Molteni, 2004: Internal variability, external forcing and climate trends in multi-decadal AGCM ensembles. *Climate. Dyn*., **23**, 659–678, https://doi.org/10.1007/s00382-004-0465-2.

Cohen, J., and M. Barlow, 2005: The NAO, the AO, and global warming: How closely related? *J. Climate*, **18**, 4498–4513.

Czaja, A., and C. Frankignoul, 2002: Observed Impact of Atlantic SST anomalies on the North Atlantic Oscillation. *J. Climate*, **15**, 606–623.

Delworth, T. L., and Coauthors, 2006: GFDL's CM2 global coupled climate models. Part I: Formulation and simulation characteristics. *J. Climate*, **19**, 643–674, https://doi.org/10.1175/JCLI3629.1.

Deser, C., A. S. Phillips, and J. W. Hurrell, 2004: Pacific interdecadal climate variability: Linkages between the tropics and the North Pacific during boreal winter since 1900. *J. Climate*, **17**, 3109–3124, https://doi.org/10.1175/1520-0442(2004)017<3109:PICVLB>2.0.CO;2.

Frankignoul, C., 1985: Sea surface temperature anomalies, planetary waves, and air–sea feedback in the middle latitudes. *Rev. Geophys*., **23**, 357–390, https://doi.org/10.1029/RG023i004p00357.

Frankignoul, C., A. Czaja, and B. L′Heveder, 1998: Air–sea feedback in the North Atlantic and surface boundary conditions for ocean models. *J. Climate*, **11**, 2310–2324, https://doi.org/10.1175/1520-0442(1998)011<2310:ASFITN>2.0.CO;2.

Gan, B. L., L. X. Wu, F. Jia, S. J. Li, W. J. Cai, H. Nakamura, M. A. Alexander, and A. J. Miller, 2017: On the response of the Aleutian low to greenhouse warming. *J. Climate*, **30**, 3907–3925, https://doi.org/10.1175/JCLI-D-15-0789.1.

Gastineau, C., and C. Frankignoul, 2015: Influence of the north Atlantic SST variability on the atmospheric circulation during the twentieth century. *J. Climate*, **28**, 1396–1416, https://doi.org/10.1175/JCLI-D-14-00424.1.

Glowienka-Hense, R., 1990: The north Atlantic oscillation in the Atlantic-European SLP. *Tellus A*, **42**, 497–507, https://doi.org/10.3402/tellusa.v42i5.11893.

Gregory, D., and P. R. Rowntree, 1990: A mass flux convection scheme with representation of cloud ensemble characteristics and stability-dependent closure. *Mon. Wea. Rev*., **118**, 1483–1506, https://doi.org/10.1175/1520-0493(1990)118<1483:AMFCSW>2.0.CO;2.

Hansen, J., R. Ruedy, M. Sato, and K. Lo, 2010: Global surface temperature change. *Rev. Geophys*., **48**, RG4004, https://doi.org/10.1029/2010RG000345.

Hao, X., F. Li, J. Q. Sun, H. J. Wang, and S. P. He, 2016: Assessment of the response of the East Asian winter monsoon to ENSO-like SSTAs in three U.S. CLIVAR Project models. *International Journal of Climatology*, **36**, 847–866, https://doi.org/10.1002/joc.4388.

Herweijer, C., and R. Seager, 2008: The global footprint of persistent extra-tropical drought in the instrumental era. *International Journal of Climatology*, **28**(13), 1761-1774, https://doi.org/10.1002/joc.1590.

Hoerling, M., A. Kumar, J. Eischeid, and B. Jha, 2008: What is causing the variability in global mean land temperature? *Geophys. Res. Lett*., **35**, L23712, https://doi.org/10.1029/2008GL035984.

Hoerling, M. P., J. W. Hurrell, T. Xu, G. T. Bates, and A. S. Phillips, 2004: Twentieth century North Atlantic climate change. Part II: Understanding the effect of Indian Ocean warming. *Climate Dyn*., **23**, 391–405, https://doi.org/10.1007/s00382-004-0433-x.

Hu, K.-M., and G. Huang, 2011: The oscillation between tropical Indian ocean and north pacific: Evidence and possible impact on winter climate in China. *Atmospheric and Oceanic Science Letters*, **4**, 57–63, https://doi.org/10.1080/16742834.2011.11446904.

Hu, Z. Z., 1997: Interdecadal variability of summer climate over East Asia and its association with 500 hPa height and global sea surface temperature. *J. Geophys. Res*., **102**, 19 403–19412, https://doi.org/10.1029/97JD01052.

Hu, Z.-Z., S. Yang, and R. G. Wu, 2003: Long-term climate variations in China and global warming signals. *J. Geophys. Res*., **108**, 4614, https://doi.org/10.1029/2003JD003651.

Hurrell, J. W., M. P. Hoerling, A. S. Phillips, and T. Xu, 2004: Twentieth century North Atlantic climate change. Part I: Assessing determinism. *Climate Dyn*., **23**, 371–389, https://doi.org/10.1007/s00382-004-0432-y.

Kalnay, E., and Coauthors, 1996: The NCEP/NCAR 40-year reanalysis project. *Bull. Amer. Meteor. Soc*., **77**, 437–471, https://doi.org/10.1175/1520-0477(1996)077<0437:TNYRP>2.0.CO;2.

Kiehl, J. T., J. J. Hack, G. B. Bonan, B. A. Boville, D. L. Williamson, and P. J. Rasch, 1998: The national center for atmospheric research community climate models: CCM3. *J. Climate*, **11**, 1131–1149, https://doi.org/10.1175/1520-0442(1998)011<1131:TNCFAR>2.0.CO;2.

Lau, N.-C., 1988: Variability of the observed midlatitude storm tracks in relation to low-frequency changes in the circulation pattern. *Journal of Atmospheric Sciences*, **45**, 2718–2743, https://doi.org/10.1175/1520-0469(1988)045<2718:VOTOMS>2.0.CO;2.

Li, S., J. Lu, G. Huang, and K. Hu, 2008: Tropical Indian ocean basin warming and east Asian summer monsoon: A multiple AGCM study. *J. Climate*, **21**, 6080–6088, https://doi.org/10.1175/2008JCLI2433.1.

Magnusdottir, G., 2001: The modeled response of the mean winter circulation to zonally averaged SST trends. *J. Climate*, **14**, 4166–4190, https://doi.org/10.1175/1520-0442(2001)014<4166:TMROTM>2.0.CO;2.

Milly, P. C. D., and A. B. Shmakin, 2002: Global modeling of land water and energy balances. Part I: The Land Dynamics (LaD)

model. *Journal of Hydrometeorology*, **3**, 283–299, https://doi.org/10.1175/1525-7541(2002)003<0283:GMOLWA>2.0.CO;2.

Mitchell, T. D., and P. D. Jones, 2005: An improved method of constructing a database of monthly climate observations and associated high-resolution grids. *International Journal of Climatology*, **25**, 693–712, https://doi.org/10.1002/joc.1181.

Moorthi, S., and M. J. Suarez, 1992: Relaxed Arakawa-Schubert: A parameterization of moist convection for general circulation models. *Mon. Wea. Rev*., **120**, 978–1002, https://doi.org/10.1175/1520-0493(1992)120<0978:RASAPO>2.0.CO;2.

Oleson, K. W., and Coauthors, 2008: Improvements to the community land model and their impact on the hydrological cycle. *J. Geophys. Res*., **113**, G01021, https://doi.org/10.1029/2007JG000563.

Peng, S. L., W. A. Robinson, and S. L. Li, 2003: Mechanisms for the NAO responses to the North Atlantic SST tripole. *J. Climate*, **16**, 1987–2004, https://doi.org/10.1175/1520-0442(2003)016<1987:MFTNRT>2.0.CO;2.

Rayner, N. A., D. E. Parker, E. B. Horton, C. K. Folland, L. V. Alexander, D. P. Rowell, E. C. Kent, and A. Kaplan, 2003: Global analyses of sea surface temperature, sea ice, and night marine air temperature since the late nineteenth century. *J. Geophys. Res*., **108**, 4407, https://doi.org/10.1029/2002JD002670.

Rodwell, M. J., D. P. Rowell, and C. K. Folland, 1999: Oceanic forcing of the wintertime North Atlantic oscillation and European climate. *Nature*, **398**, 320–323, https://doi.org/10.1038/18648.

Schneider, E. K., L. Bengtsson, and Z.-Z. Hu, 2003: Forcing of northern hemisphere climate trends. *Journal of Atmospheric Sciences*, **60**, 1504–1521, https://doi.org/10.1175/1520-0469(2003)060<1504:FONHCT>2.0.CO;2.

Shin, S. I., and P. D. Sardeshmukh, 2011: Critical influence of the pattern of Tropical Ocean warming on remote climate trends. *Climate Dyn*., **36**, 1577–1591, https://doi.org/10.1007%2Fs00382-009-0732-3.

Sutton, R. T., W. A. Norton, and S. P. Jewson, 2000: The North Atlantic oscillation—What role for the ocean? *Atmospheric Science Letters*, **1**, 89–100, https://doi.org/10.1006/asle.2000.0018.

Ueda, H., Y. Kamae, M. Hayasaki, A. Kitoh, S. Watanabe, Y. Miki, and A. Kumai, 2015: Combined effects of recent Pacific cooling and Indian Ocean warming on the Asian monsoon. *Nature Communications*, **6**, 8854, https://doi.org/10.1038/ncomms9854.

Visbeck, M., E. P. Chassignet, R. G. Curry, T. L. Delworth, R. R. Dickson, and G. Krahmann, 2003: The ocean's response to North Atlantic oscillation variability. *The North Atlantic Oscillation*: *Climatic Significance and Environmental Impact*, J. W. Hurrell et al., Eds., *Geophysical Monograph*, Vol. 134, American Geophysical Union, 113–145, https://doi.org/10.1029/134GM06.

Wallace, J. M., C. Smith, and Q. R. Jiang, 1990: Spatial patterns of atmosphere–ocean interaction in the Northern Winter. *J. Climate*, **3**, 990–998, https://doi.org/10.1175/1520-0442(1990)003<0990:SPOAOI>2.0.CO;2.

Watanabe, M., and M. Kimoto, 2000: Atmosphere-ocean thermal coupling in the North Atlantic: A positive feedback. *Quart. J. Roy. Meteor. Soc*., **126**, 3343–3369, https://doi.org/10.1002/qj.49712657017.

Xie, S.-P., C. Deser, G. A. Vecchi, J. Ma, H. Y. Teng, and A. T. Wittenberg, 2010: Global warming pattern formation: Sea surface temperature and rainfall. *J. Climate*, **23**, 966–986, https://doi.org/10.1175/2009JCLI3329.1.

Zhang, G. J., and N. A. McFarlane, 1995: Sensitivity of climate simulations to the parameterization of cumulus convection in the Canadian Climate Centre general circulation model. *Atmos.-Ocean*, **33**, 407–446, https://doi.org/10.1080/07055900.1995.9649539.